Chemosphere 216 (2019) 698–706

Contents lists available at ScienceDirect

Chemosphere

journal homepage: www.elsevier.com/locate/chemosphere

Influence of pyrolysis temperature on characteristics and environmental risk of heavy metals in pyrolyzed biochar made from hydrothermally treated sewage sludge

Xingdong Wang [a], Qiaoqiao Chi [a], Xuejiao Liu [a, b], Yin Wang [a, *]

[a] CAS Key Laboratory of Urban Pollutant Conversion, Institute of Urban Environment, Chinese Academy of Sciences, Xiamen 361021, China
[b] University of Chinese Academy of Sciences, Beijing 100049, China

HIGHLIGHTS

- Hydrothermally treated sewage sludge was pyrolyzed to form biochar.
- Pyrolysis temperature had a significant effect on biochar properties.
- Combining hydrothermal pretreatment with pyrolysis immobilizes heavy metals.
- High-temperature pyrolysis can reduce the ecological risk from HMs in biochar.

GRAPHICAL ABSTRACT

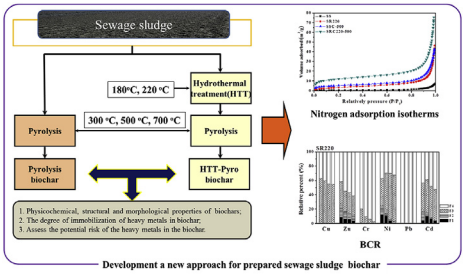

ARTICLE INFO

Article history:
Received 7 May 2018
Received in revised form
21 September 2018
Accepted 27 October 2018
Available online 30 October 2018

Handling Editor: Chang-Ping Yu

Keywords:
Sewage sludge biochar
Hydrothermal treatment
Pyrolysis
Heavy metals
Risk assessment

ABSTRACT

A novel approach was used to prepare sewage sludge (SS)-derived biochar via coupling of hydrothermal pretreatment with pyrolysis (HTP) process at 300–700 °C. The influence of the pyrolysis temperature on the characteristics and environmental risk of heavy metals (HMs) in biochar derived from SS were investigated. The HTP process at higher pyrolysis temperature (≥500 °C) resulting in a higher quality of SS-derived biochar and in HMs of lower toxicity and environmental risk, compared with direct SS pyrolysis. Surface characterization and micromorphology analysis indicate that the N_2 adsorption capacity and BET surface area in biochar (SRC_{220}-500) obtained from hydrothermally treated SS at 220 °C (SR_{220}) pyrolysis at 500 °C, significantly increased the BET surface area and achieved its maximum value (47.04 m^2/g). Moreover, the HTP process can promote the HMs in SS be transformed from bioavailable fractions to more stable fractions. This increases with the pyrolysis temperature, resulting in a remarkable reduction in the potential environmental risk of HMs from the biochar obtained from the HTP process.

1. Introduction

Large amounts of sewage sludge (SS) are generated from municipal wastewater treatment plants in China. The predicted rate of increase is about 10% per year over a ten-year period (Zhang et al., 2014; Garlapalli et al., 2016; Havukainen et al., 2017) due to current rapid economic development and urbanization. Such situation has become a disturbing waste problem all around the world, because SS contains numerous harmful organic and inorganic substances, such as hazardous organic micro-pollutants, pesticides,

* Corresponding author.
E-mail address: yinwang@iue.ac.cn (Y. Wang).

https://doi.org/10.1016/j.chemosphere.2018.10.189
0045-6535/

herbicides, pathogens, and heavy metals (HMs) (Leng et al., 2016; Liu et al., 2017). However, SS can also be considered a bio-resource because of its high content of biodegradable organic matter (He et al., 2013; Peng et al., 2016). Conventional SS disposal technologies include landfill, land application, and incineration (Chen et al., 2012). Landfill and direct land application generates undesired emissions (e.g., HMs and pathogens) to soil and water, and the accumulated soil and water pollution with HMs, may easily result in unintended harm to humans and wildlife (Schwarzenbach et al., 2006). On the other hand, incineration is gradually being prohibited due to its production of secondary pollution, high operational cost, and newly more stringent regulations. Therefore, it is crucial to explore economically feasible and environment-friendly technology to combine facilitation of waste recycling and reduction of the environmental risk of HMs in SS.

Alternatively, pyrolysis has been proven a promising approach for stabilization and resource utilization of SS owing to the ease and efficiency by which it can be performed. Pyrolysis can significantly minimize the volume of SS, kill parasites and pathogens, reduce the organic pollutants contents, and immobilize HMs in the biochar derived from pyrolysis at high temperature (Devi and Saroha, 2014). It can also, more importantly, be used to convert effectively most of organic matter to bio-energy fuels (e.g., gases and bio-oils) and high-quality biochar (Mendez et al., 2014). The biochar, in particular, has been gathering increased attention for use in soil fertility enhancement, soil remediation, and pollution removal from aqueous solutions as a cost-effective sorbent (Chen et al., 2008a; Sohi, 2012; Xiao and Chen, 2017). Previous studies have shown that the SS biochar can be used as a soil ingredient to increase the cation exchange capacity, pH value, water holding capacity of soil, and to improve soil fertility. For example, Khan et al. (2013) proposed the addition of SS biochar to soil to mitigate climate change, increase soil fertility, and minimize bioaccumulation of toxic metals. Yue et al. (2017) investigated the efficiency of SS biochar for improving poor urban soil properties and promoting grass growth. They proposed that SS biochar be used in poor urban raw soil as a soil conditioner. However, the environmental risk from HMs accumulated in biochar must be carefully considered to provide adequate safety with future large-scale application. Various researchers have reported on the mobility of HMs in biochar derived from SS. Kistler et al. (1987) investigated the mobility behavior of HMs (Cr, Ni, Cu, Zn, Cd, Pb, and Hg) in SS during pyrolysis and found that the HMs in biochar were significantly immobile due to its alkaline properties. Devi and Saroha (2014) observed that major HMs (Cd, Cr, Cu, Ni, Pb, and Zn) were enriched in the biochar matrix. However, the bioavailability and eco-toxicity of the HMs in the biochar were significantly reduced after pyrolysis.

The abovementioned pyrolysis experiments were conducted using dried SS feedstock, so cost-effective pretreatment and dewatering processes were required. Hydrothermal treatment is a method in which SS can be heated in the autoclave reactor and the extracellular polymeric substances (EPSs) in SS are decomposed to release the bound water, leading to an improvement of SS dewaterability (Bougrier et al., 2008). It has been widely investigated as a way to de-water moist SS due to its effectiveness and simplicity (Akiya and Savage, 2002; Wang et al., 2016). It causes the solubilization and disruption of flocs contained in the EPS of wet SS so as to the release its bound water, thus leading to improvement in the SS dewaterability (Bougrier et al., 2008). Furthermore, treatment of SS in supercritical water can also stabilize the HMs that it contains (Shi et al., 2013). Previous studies indicate that the HMs in SS could be transformed from bioavailable fractions to more stable fractions, although the majority of the HMs accumulated in the solid residue after hydrothermal treatment (Yuan et al., 2011a,b; Leng et al., 2014; Leng et al., 2016). Therefore, it has been demonstrated that pyrolysis and hydrothermal treatment could lead to a significant enhancement of the stabilization of HMs in the SS biochar product. In a previous study, we developed a novel technology coupling hydrothermal pretreatment with solid residual pyrolysis (HTP) for treatment/disposal of SS (Wang et al., 2016). After the HTP process, dehydration performance was significantly enhanced, and the leaching potential of the HMs was also reduced compared with hydrothermal treatment or pyrolysis of SS alone, thus decreasing the environmental risk involved in the application of SS biochar. Therefore, HTP is considered an appropriate method for disposal of SS by preparation of biochar.

To date, little information has become available regarding the physical and chemical properties of SS biochar derived from the HTP process, and the effect of the pyrolysis temperature on immobilization of HMs in SS biochar derived from the HTP process remains unclear. Hence, the objectives of the this work were (1) to investigate the effects of the HTP process and pyrolysis temperature on biochar physicochemical and surface properties, (2) to reveal the degree of immobilization of HMs in biochar in relation to different pyrolysis temperatures during the HTP process, and (3) to assess the potential risk of the HMs in the biochar.

2. Materials and methods

2.1. Materials

Wet SS (moisture content 85.25 wt.%) was obtained from a municipal wastewater treatment plant in Xiamen (Fujian Province, China). The SS was shaken and mixed thoroughly; then kept at 4 °C in a refrigerator until the hydrothermal treatment tests. A SS sample was dried for 24 h at 105 °C in an oven, ground into fine particles (0.043–0.15 mm), and then stored in a desiccator to maintain its low water content against the ambient humidity. The main characteristics of the SS are listed in Table 1.

2.2. Experimental procedure

The hydrothermal treatment experiments were conducted in an electrically heated autoclave reactor with a working volume of 2 L, maximum temperature of 400 °C and maximum pressure of 30 MPa (see Fig. S1a). In each batch experiment, approximately 1000 g of the dewatered SS and 200 mL of deionized water were loaded into the internal vessel and sealed. Then, 99.99% pure argon was supplied from a cylinder into the reactor to create oxygen-free conditions. The reactor was then placed in an electrically heated furnace and heated to the target temperature (180 and 220 °C), under autogenous pressure. When the target temperature was reached, treatment was continued for 30 min. During the reaction, the sample was continually stirred at 200 rpm to ensure that the temperature was uniform throughout the sample. After the hydrothermal treatment process, the mixed liquid was poured out of the reactor owing to the greatly enhanced dewatering of the SS. Then, the solid residue (SR) was separated using laboratory-scale plate-frame pressure filtration. The SR obtained was subsequently dried in a beaker at 105 °C for at least 24 h and weighed to obtain the weight of the SR sample. The SR samples were labeled as SR_X, where X referred to the hydrothermal treatment temperature. All hydrothermal treatment tests were performed in triplicate.

A schematic diagram of the pyrolysis apparatus is shown in Fig. S1(b). Pyrolysis of the SS and SRs were carried out according to the procedure reported in our previous publication (Han et al., 2014). In each pyrolysis test, 15.0 g of dried SS/SR was first inserted into a quartz tube, through which argon gas of 99.99% purity was purged for 1 h to flush out the oxygen before starting pyrolysis.

Table 1
Physicochemical properties of the SS, SRs and their biochar samples obtained at different pyrolysis temperature.

Samples	Yield (%)	pH	Ash (%)	C (%)	H (%)	N (%)	S (%)	O[a] (%)	H/C	O/C	N/C
SS	/	6.82 ± 0.15	46.62 ± 1.25	24.67 ± 0.55	4.65 ± 0.19	4.51 ± 0.13	0.95 ± 0.03	18.60	2.26	0.57	0.16
SSC-300	68.65 ± 1.35	7.02 ± 0.27	63.97 ± 2.55	21.16 ± 0.43	2.30 ± 0.20	3.35 ± 0.09	1.00 ± 0.09	8.22	1.30	0.29	0.14
SSC-500	60.07 ± 0.79	7.70 ± 0.22	77.44 ± 1.99	15.61 ± 0.13	0.86 ± 0.02	2.20 ± 0.04	0.62 ± 0.01	3.26	0.66	0.16	0.12
SSC-700	56.11 ± 1.44	8.89 ± 0.39	81.15 ± 1.90	15.32 ± 0.17	0.47 ± 0.01	1.38 ± 0.03	0.56 ± 0.02	1.12	0.37	0.05	0.08
SR_{180}	/	6.01 ± 0.19	58.04 ± 0.93	20.34 ± 0.09	3.65 ± 0.08	2.84 ± 0.15	0.86 ± 0.04	14.27	2.15	0.53	0.12
SRC_{180}-300	80.89 ± 2.09	6.51 ± 0.25	68.62 ± 2.31	17.69 ± 0.30	2.14 ± 0.18	2.28 ± 0.33	1.17 ± 0.01	8.10	1.45	0.34	0.11
SRC_{180}-500	67.79 ± 1.17	7.54 ± 0.30	81.55 ± 2.07	11.91 ± 0.15	0.71 ± 0.06	1.43 ± 0.10	0.85 ± 0.02	3.54	0.72	0.22	0.10
SRC_{180}-700	65.39 ± 0.59	8.51 ± 0.11	85.56 ± 0.71	11.60 ± 0.09	0.42 ± 0.02	0.85 ± 0.02	0.90 ± 0.06	0.68	0.44	0.04	0.06
SR_{220}	/	6.47 ± 0.32	62.35 ± 0.83	18.77 ± 0.11	3.08 ± 0.08	2.20 ± 0.17	0.86 ± 0.04	12.74	1.97	0.51	0.10
SRC_{220}-300	86.66 ± 2.06	6.57 ± 0.09	69.97 ± 1.22	17.48 ± 0.07	2.24 ± 0.13	2.01 ± 0.03	1.47 ± 0.07	6.82	1.54	0.29	0.10
SRC_{220}-500	73.25 ± 1.13	7.51 ± 0.17	82.55 ± 1.36	11.15 ± 0.24	0.82 ± 0.07	1.24 ± 0.12	1.11 ± 0.02	3.14	0.88	0.21	0.09
SRC_{220}-700	70.83 ± 0.79	8.52 ± 0.30	86.35 ± 2.04	10.78 ± 0.19	0.46 ± 0.04	0.80 ± 0.03	1.05 ± 0.04	0.57	0.51	0.04	0.06

SS, sewage sludge; SR_X, the solid residue obtained from hydrothermal treatment sewage sludge at X (°C) temperature; SSC-Y, biochar derived from sewage sludge pyrolysis at Y (°C) temperature; SRC_X-Y, biochar derived from hydrothermally treated sewage sludge at X (°C) pyrolysis at Y (°C) temperature.
Values are the mean ± SD (standard deviation) of three replicated tests.
[a] By difference, O = 100 − (C + H + N + S + Ash).

An argon gas flow rate of 100 mL min^{-1} was maintained during the entire pyrolysis process. The pyrolysis temperature was raised from room temperature to 300, 500, or 700 °C at a rate of 15 °C·min^{-1}, and then the target temperature was maintained for 40 min. The resultant biochars obtained from SS and SRs at various temperatures were noted as SSC-Y and SRC_X-Y, respectively, where X referred to the hydrothermal treatment temperature and Y referred to the pyrolysis temperature. The biochar produced in each case was stored in a desiccator until later use. All pyrolysis experiments were replicated in triplicate.

2.3. Characterization of biochar

The total content of C, H, N, and S in the SS, SR, and SS-biochar samples were analyzed with an elemental analyzer (VARIO MAX, Germany). The pH of the SS, SR, and biochar samples (sample to water = 1:20, W/V) were measured with a pH meter (Denver, UB-7, USA). The sample BET surface area and porosity were determined using N_2 adsorption-desorption isotherms at 77 K with a surface apparatus (Micromeritics ASAP 2020). The surface functional groups of the samples were obtained using FTIR spectrometry. The oven-dried samples were mixed with KBr (1:100) in an agate mortar, and the resulting mixed powder was pressed into pellets for analysis. Spectra were recorded in the range 400–4000 cm^{-1} at a resolution of 4 cm^{-1}.

2.4. Analysis of HMs

2.4.1. Fraction procedure of HMS

The HMs (Cu, Zn, Cr, Ni, Pb, and Cd) in the SS, SR, and biochar samples were sequentially extracted using the three-step BCR sequential extraction procedure. This procedure apportions the HMs into four fractions: acid soluble/exchangeable fraction (F1), reducible fraction (F2), oxidizable fraction (F3), and residual fraction (F4), according to the Commission of the European Communities Bureau of Reference. The details of the BCR sequential extraction procedure were reported by Chen et al. (2014). For F1–F3, the suspension was collected after each step by centrifugation at 6000 rpm for 20 min in a centrifuge and filtered through a 0.22-μm nylon filter. The resultant filtrate was then diluted to a constant volume (50 mL) with HNO_3 (2%). The diluted filtrate samples were digested with mixed acid (H_2O_2/HNO_3) to remove dissolved organics. F4 and the total content of HMs in the samples were determined after digestion with a microwave digestion system with an acid mixture (HNO_3: $HClO_4$: HF = 5: 5: 2, v/v). Each of the digestion solutions was filtered through a 0.22 μm nylon filter to remove fine particles before analysis. Then, the HM (Cu, Zn, Cr, Ni, Pb, and Cd) content in each digestion solution was analyzed using ICP-MS (Agilent Technologies, 7500CX, Santa, Clara, CA). All experiments were conducted in triplicate and the results were expressed only as mean values ± SD (standard deviation).

2.4.2. Evaluation of risk assessment code (RAC)

Risk assessment code (RAC) was employed to assess the environment risk of HMs in SS, SRs, and biochars, It has been widely used in the environment science for heavy metal toxicity assessment (Shi et al., 2013; Leng et al., 2016). RAC assesses the available of HMs in SS, SRs, and biochars by applying the percentage of HMs present in F1 fraction. Five classification of RAC were showed as: no risk (NR), RAC lower than 1%; low risk (LR), RAC in the range of 1–10%; medium risk (MR), RAC in the range of 11–30%; high risk (HR), RAC in the range of 31–50%; very high risk (VHR), RAC higher than 50% (Zhai et al., 2014).

2.4.3. Potential ecological risk index (RI)

Potential ecological risk index (RI) proposed by Hakanson (1980), based on the total concentration, number, toxicity and sensitivity of HMs was used to evaluate the degree of potential risk of HMs pollution in SS and biochars using the following equations:

$$C_f = C_m/C_n \quad (1)$$

$$E_r = T_r \times C_f \quad (2)$$

$$RI = \sum E_r \quad (3)$$

where, C_f is the individual HM contamination factor; C_m and C_n are the potential mobile fractions (F1+F2+F3) and stable fraction (F4) of the HMs respectively; E_r is the potential ecological risk factor for individual HM; T_r is toxic factor of the individual HM, the values for each HM are in the order of Zn (1), Cr (2), Cu (5), Ni (6), Pb (5), and Cd = 30 (Hakanson, 1980); RI is the potential ecological risk index of the overall contamination. The values of C_f, E_r and RI can be used to the risk evaluation of HMs in SS, SRs, and biochars.

3. Results and discussion

3.1. General properties of the biochars

The major properties, including the biochar yield, pH, ash content, and elemental composition of SS, SRs, and biochar products

are summarized in Table 1. The percentage of biochar yield for SSC declined steadily from 68.65 to 58.11% with increase in the pyrolysis temperature from 300 to 700 °C. This was owing to the massive decomposition of organic substances in the SS during pyrolysis. The pyrolysis of SRs led to a greater increase in the biochar yield due to the higher ash content of SRs (58.04% for SR_{180} and 62.35% for SR_{220}, but 45.62% for SS). It can be seen that the biochar yield greatly depended on the inorganic constituents in the original feedstock. In this study, the content of main inorganic present in the SS were 19.51, 8.05, 43.07, 13.14, 1.14, and 5.71 g kg^{-1} for P, K, Fe, Al, Ca, and Na, respectively. Similar results have been reported by other researchers (Agrafioti et al., 2013; Chen et al., 2014). The pH of SS was close to neutral. The hydrothermal treatment of the SS first increased the acidity of SR_{180} (by 6.01%) due to the degradation of macromolecules into acidic substances at relatively low temperature; then, the pH of SR_{220} increased (6.47%) with the treatment temperature. This change could be linked to the degradation of acidic substances and decomposition of proteins at higher temperatures (Funke and Ziegler, 2010). During the pyrolysis process, the alkali salts in the ash of SS/SR were released from the pyrolytic structure and the amount of acidic surface-functional groups decreased with oxygen percentage losses at higher pyrolysis temperatures (Yuan et al., 2011a; Zheng et al., 2013). This resulted in gradual increase in the pH of the biochar (from neutral or acid to alkaline) with increase in the pyrolysis temperature.

The content of C, H, N, and O in the biochar derived from SS/SR decreased with increase in the pyrolysis temperature from 300 to 700 °C (Table 1). It can be seen that the S content of biochar was relatively constant despite change of the pyrolysis temperature. The molar ratios of H/C and O/C are major carbonization-degree parameters that are generally used to characterize the degree of organic aromaticity of the biochar. Both ratios (H/C and O/C) of the biochar declined significantly with increasing pyrolysis temperature, leading to far greater carbonization and higher aromatic condensation (Chen et al., 2014; Cayuela et al., 2015). Biochar with higher aromaticity is resistant to decomposition in soil for many years, meaning that the biochar created at higher pyrolysis temperature would have greater stability in the soil environment (Huang et al., 2017). The trend of the molar ratio of N/C in the biochar was similar to the molar ratios of H/C and O/C. This indicates that N-related functional groups on the biochar surfaces were gradually reduced with increase in the pyrolysis temperature from 300 to 700 °C. That is to say, there should be less organic-N leached from the soil when this biochar is incorporated into soil, compared with the application of raw sewage sludge (Qayyum et al., 2014).

3.2. Functional group analysis

The FTIR spectra of SS, SRs, and biochar samples formed at different pyrolysis temperatures are presented in Fig. 1. The FTIR spectra of SS and SRs were similar, suggesting hydrothermal treatment did not lead to significant changes of the main functional groups due to its moderation and stability. This was consistent with a previous reported by Peng et al. (2016). The intensity of the peak around 3400 cm^{-1} was attributed to hydroxyl functionalities (the vibration of −OH stretching) and the intensity of −OH stretching decreased in the steps from SS to SRs to biochar. This indicates that

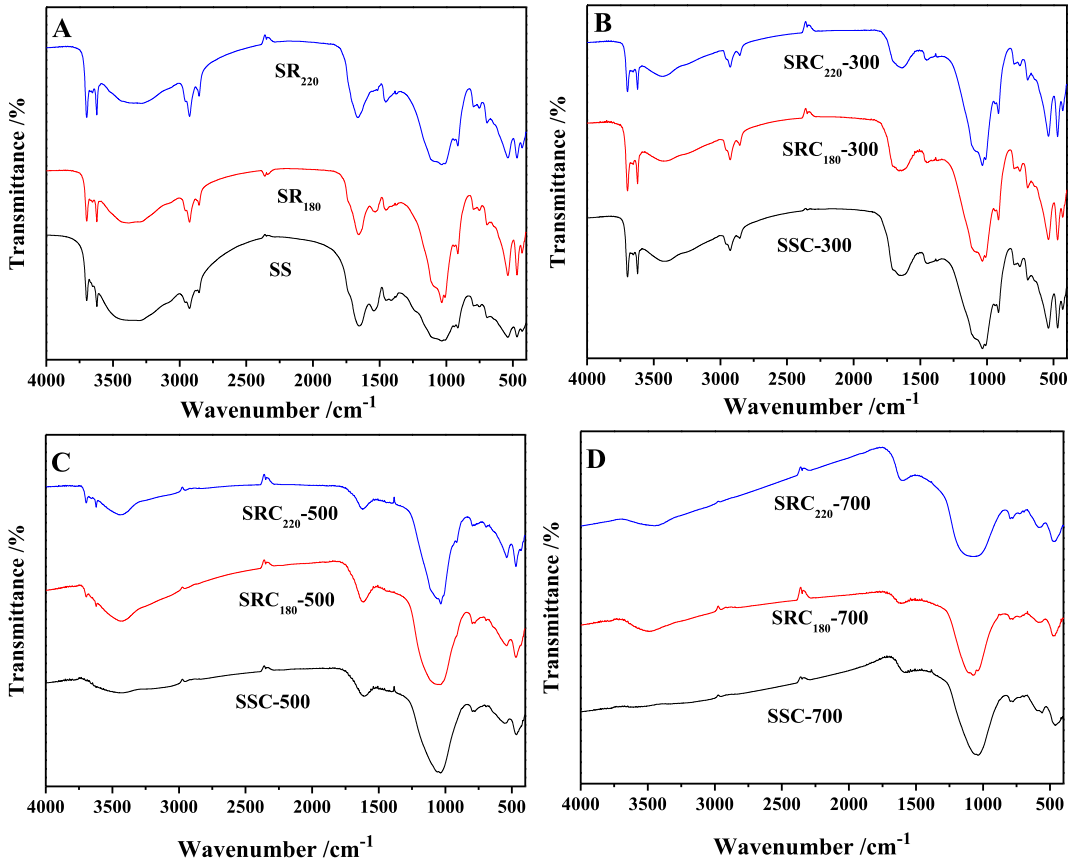

Fig. 1. FTIR spectra of (A) SS and SRs, (B) Biochars formed at 300 °C, (C) Biochars formed at 500 °C, and (D) Biochars formed at 700 °C. SS, sewage sludge; SR_X, the solid residue obtained from hydrothermal treatment sewage sludge at X (°C) temperature; SSC-Y, biochar derived from sewage sludge pyrolysis at Y (°C) temperature; SRC_X-Y, biochar derived from hydrothermally treated sewage sludge at X (°C) pyrolysis at Y (°C) temperature.

the dehydration and dehydroxylation capacities of SS were improved during hydrothermal treatment and subsequent pyrolysis. This led to decomposition of large numbers of the hydroxyl groups in SS. Moreover, it is noteworthy that the peak above 3600 cm^{-1} may refer to –OH groups of alcohols (Huang et al., 2017), which were not detected at pyrolysis temperature higher than 500 °C. Moreover, the peak around 2800–3000 cm^{-1} that was attributed to aliphatic CH_n groups (C–H stretching), disappeared abruptly upon heating at higher pyrolysis temperature (i.e. ≥ 700 °C). The results show that organic fatty hydrocarbons were decomposed to carbon dioxide, methane, and other gases, or transformed into aromatic structures (Lu et al., 2013). The peaks at 1603–1625 cm^{-1} reflect amide bonds and aromatic ring stretching (C=O, –CONH–, and C=C stretching vibration) (Jin et al., 2016), and their intensity decreased a bit with rise in the pyrolysis temperature. The changes of these functional groups indicate that biochar possess a structure in which aromatic carbon compounds play a central role. The 1415 cm^{-1} peak (CH_3 and CH_2 groups) disappeared when the pyrolysis temperature reached 500 °C because of the decomposition of chain hydrocarbons.

The strong peak at 1036 cm^{-1} was associated with the band for C–O–C aliphatic/ether stretching, which exhibited only a slight change irrespective of the pyrolysis temperature. This was because the different forms of oxygen in raw sewage sludge were transformed into carbon chains with carbon–oxygen single bonds during the SS pyrolysis process (Ho et al., 2017). The low-intensity peaks between 670 and 800 cm^{-1} were assigned to aromatic groups and hetero-aromatic compounds (Hossain et al., 2011; Huang et al., 2017). The aromatic groups can provide π-electrons, which have been found to have the potential to bond strongly with heavy metal cations (Harvey et al., 2011). The bands below 600 cm^{-1} were metal-halogen stretching vibrations in both organic and inorganic halogen compounds (Hossain et al., 2011; Huang et al., 2017).

3.3. Surface characterizations and micromorphology

Fig. 2 illustrates the N_2 adsorption isotherms of SS, SR_{220}, SSC-500, and SRC_{220}-500. SRC_{220}-500 exhibited higher N_2 adsorption capacity compared with SS, SR_{220}, and SSC-500. This result indicates that the SRC_{220}-500 had the structure with the most abundant pores. The BET surface area, pore size, and total pore volume of the SS, SRs, and their biochars obtained under different pyrolysis temperature, are displayed in Table S1, and the results show that the surface area, pore size, and total pore volume were largely dependent on the hydrothermal treatment temperature and pyrolysis temperature. In contrast to biochars, SR_{180} and SR_{220} had relatively lower surface area and total pore volume because the SRs obtained from SS hydrothermal treatment usually exist in the form of amorphous macro spheres with very low microporosity (Reza et al., 2014; Mumme et al., 2015). Garlapalli et al. (2016) observed similar results and reported that intermediates in the SRs are trapped or adsorbed to the surface, resulting in further reduction of the BET surface area. However, as the pyrolysis temperature was elevated from 300 to 700 °C, the surface area of the SS biochar clearly increased from (1.86–22.17) m^2/g and the pore volume from (0.0112–0.0628) cm^3/g. Furthermore, when the pyrolysis temperature increased from 300 to 500 °C, the surface area and pore volume of the SR biochar increased significantly and the surface area reached the theoretical maximum (47.04 m^2/g for SRC_{220}-500). Such remarkable increase of the surface area and pore volume might be from the release of volatile components in SR. However, the surface area and pore volume of SRC_{180}-700 and SRC_{220}-700 showed a trend of decrease that might be ascribed to pore blockage in the SR biochar at higher reaction temperature (Li et al., 2017).

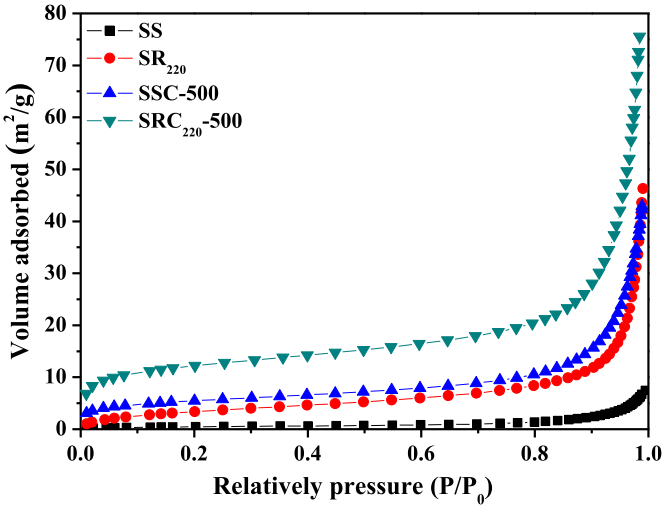

Fig. 2. Nitrogen adsorption isotherms of SS, SR_{220}, SSC-500, and SRC_{220}-500. SS, sewage sludge; SR_{220}, the solid residue obtained from hydrothermal treatment sewage sludge at 220 °C; SSC-500, biochar derived from sewage sludge pyrolysis at 500 °C; SRC_{220}-500, biochar derived from hydrothermally treated sewage sludge at 220 °C pyrolysis at 500 °C temperature.

3.4. HMs analysis

3.4.1. Total concentrations of metal HMs in the SS and its biochars

The total concentrations of Cu, Zn, Cr, Ni, Pb, and Cd in raw SS, SR, and the biochar samples are listed in Table 2. The threshold values of HMs cited from the disposal standards of pollutants for landscaping sludge in China (MEP of China, GB 32486-2009) are also listed in Table 2. It can be observed that the total concentrations of HMs in the SS, SRs, and their biochars followed the sequence Cu > Zn > Cr > Ni > Pb > Cd. The SS sample had very high concentrations of Cu, Zn, Cr, and Ni, but relatively low concentrations of Pb and Cd. Comparing these and the threshold values, the total contents of Cu, Cr, and Ni in SS all far exceeded the control range (regulatory limit) for neutral and alkaline soils (pH ≥ 6.5). In the SS, Zn slightly exceeded the acid soil (pH < 6.5) limit, and Pb and Cd in SS were lower than the acid soil (pH < 6.5) limit. The high concentration of Cu, Zn, and Cr in SS may restrict its application for landscaping. Table 2 shows that the total concentrations of HMs in the SRs gradually increased with increase in the hydrothermal treatment temperature. This increase can be attributed to the enrichment of the HMs in SS in the SR when simultaneous extraction and stabilization occur during the hydrothermal treatment process. Furthermore, the total concentrations of Cu, Zn, Cr, Ni, and Pb found in SS and SR, were partitioned in the biochar during the pyrolysis process and increased with increasing pyrolysis temperature. The result was that the total concentrations of Cu, Zn, Cr, Ni, and Pb in the biochar were higher than those in the SS and SRs (Table 2).

The distributions of HMs in biochar and bio-oil were displayed in Table S2. It was noted that Cu, Zn, Cr, Ni and Pb distributed in biochar were over 87.48%, only a small amount of them were observed in the liquid bio-oils and gas, possibly owing to the lower loss in weight of heavy metals than the loss in weight of organic compounds during pyrolysis. This can be explained by the decomposition of organic matter in the SS during pyrolysis process, resulting in the release of HMs bound to the organic matter, then co-precipitated within the biochar matrix. In particular, the Cd content in the biochars was greatly increased with increase of the pyrolysis temperature from 300 to 500 °C. However, when the

Table 2
Total concentrations of HMs in samples and their threshold values in the disposal standards of China.

Sample	Heavy metals (mg· kg^{-1}) [a]					
	Cu	Zn	Cr	Ni	Pb	Cd
SS	3323.9 ± 33.5	2424.2 ± 33.7	1983.8 ± 19.7	422.0 ± 7.5	69.7 ± 0.7	1.65 ± 0.04
SSC-300	4423.7 ± 13.6	3237.6 ± 29.3	2686.2 ± 14.3	537.8 ± 7.2	97.2 ± 0.6	2.25 ± 0.03
SSC-500	5265.7 ± 25.1	3791.3 ± 53.4	3082.0 ± 10.3	647.7 ± 3.5	110.4 ± 0.5	2.49 ± 0.05
SSC-700	5513.0 ± 8.4	3925.9 ± 23.7	3317.1 ± 21.6	671.6 ± 7.2	114.8 ± 0.5	0.45 ± 0.01
SR_{180}	4042.9 ± 4.2	2943.5 ± 66.9	2391.6 ± 59.7	450.5 ± 10.4	85.7 ± 0.2	1.91 ± 0.03
SRC_{180}-300	4853.8 ± 3.3	3445.2 ± 77.4	2838.9 ± 66.6	527.0 ± 2.5	101.1 ± 0.2	2.33 ± 0.04
SRC_{180}-500	5780.6 ± 17.8	3834.4 ± 16.5	3199.7 ± 103.6	611.7 ± 1.9	116.0 ± 0.1	2.78 ± 0.04
SRC_{180}-700	6168.9 ± 114.3	4128.6 ± 8.5	3435.2 ± 38.5	689.0 ± 0.8	130.8 ± 0.2	1.04 ± 0.02
SR_{220}	4439.8 ± 73.1	3203.6 ± 68.4	2609.3 ± 49.6	480.4 ± 10.5	94.0 ± 0.2	2.06 ± 0.03
SRC_{220}-300	5064.0 ± 39.1	3513.5 ± 84.7	2957.7 ± 61.6	536.4 ± 1.5	104.3 ± 0.1	2.35 ± 0.04
SRC_{220}-500	5940.5 ± 66.1	4058.2 ± 91.6	3269.8 ± 65.1	639.7 ± 1.6	123.2 ± 0.2	2.75 ± 0.04
SRC_{220}-700	6258.7 ± 45.5	4321.3 ± 8.0	3485.0 ± 9.5	709.9 ± 1.4	131.8 ± 0.7	1.88 ± 0.03
Threshold values [b]						
China pH < 6.5	800	2000	600	100	300	5
China pH ≥ 6.5	1500	4000	1000	200	1000	20

SS, sewage sludge; SR_X, the solid residue obtained from hydrothermal treatment sewage sludge at X (°C) temperature; SSC-Y, biochar derived from sewage sludge pyrolysis at Y (°C) temperature; SRC_X-Y, biochar derived from hydrothermally treated sewage sludge at X (°C) pyrolysis at Y (°C) temperature.
[a] The concentration of HMs is the mean concentration ± SD (standard deviation).
[b] According to the MEP of China (GB 32486-2009).

temperature was steadily increased to 700 °C, the Cd contents in the biochar decreased rapidly, indicating that a large fraction of the Cd in SS/SRs was partitioned into the bio-oil and gas when the temperature reached 700 °C (Table S2) (Kistler et al., 1987; Chen et al., 2014; Devi and Saroha, 2014). Cd existed mainly as carbonate in the SS and SR, and may have volatilized into the gas stream (Hayes and Theis, 1978). From there, it would have been released by off-gassing when the pyrolysis temperature reached 600 °C (Kistler et al., 1987). The above results indicated that the total HMs content (except for Cd in biochars formed at 700 °C) in SRs, SS-biochar, and SR-biochar was higher than that in raw SS, and followed the order SRC > SSC > SR. This suggests that the three methods (hydrothermal treatment, pyrolysis, and HTP) all allowed significant amounts of HMs in the SS, to accumulate in solid samples, and that the concentrations of these increased with increasing temperature. The accumulation of HMs in biochar appears to indicate a higher environmental risk than those in SS when only the total HMs concentrations are considered for assessment. However, the bioavailability and toxicity of HMs in the environment mainly depend on their chemical species rather than their absolute quantity (Yuan et al., 2011b; Huang and Yuan, 2016).

3.4.2. Speciation of HMs in the SS and its biochars

The modified BCR method was used to determine the chemical speciation of HMs in the SS, SR, and biochar samples. By this method, the HMs were apportioned into four fractions: F1 (the acid soluble/exchangeable fraction); F2 (the reducible fraction); F3 (the oxidizable fraction); and F4 (the residual fraction) (Chen et al., 2008b; Devi and Saroha, 2014; Leng et al., 2014). The (environmental) immobility of the HM fractions is expressed in the order: F4 > F3 > F2 > F1. The fractions are also divided into three categories (Huang and Yuan, 2016): the metals in the F1 and F2 fractions are recognized as species that are directly toxic; the F3 fraction is a potentially toxic fraction because its members are easily degraded; and the F4 fraction is recognized as non-toxic (Devi and Saroha, 2014).

In fact, the total concentration of HMs obtained from the acid digestion procedure must equal to the sum of the HMs content of each fraction determined in the BCR sequential extraction procedure. As a check on the results from the BCR procedure, the sum of the four fractions (F1, F2, F3 and F4) and the total concentration of HMs determined by the acid digestion procedure were compared in the following equation:

$$R(\%) = \frac{F1 + F2 + F3 + F4}{TC} \times 100 \quad (4)$$

where, R is the percentage recovery of HMs (%); F1, F2, F3, and F4 are the HM content in each fraction (mg kg^{-1}); and TC is the total content of HM (mg kg^{-1}). The results for the evaluation of this method are shown in Table S3, and good agreement exists between the two HM concentrations from procedures with satisfactory recovery (95.3–106.1%).

Fig. 3 indicates the speciation of the HMs in the SS, SRs, and their biochars formed at different pyrolysis temperatures. The main distribution patterns of the HMs in SS and SRs were found to be different. The content of the F1 and F2 fractions of Cu, Cr, and Pb were very low in SS (especially for Cr and Pb, which were near zero). This suggests less environmental risk from Cu, Cr, and Pb in raw SS. The Cu in SS was predominantly in the F3 fraction (67.02%) due to its high-stability Cu-organic matter complexes (Staelens et al., 2000; Shi et al., 2013). The Cr and Pb in SS were mainly present in the F4 fraction (66.27 and 99.97%). Similar results were reported by Wong et al. (2001), indicating that over 90% of the Cr in raw SS was accounted for in the organic and residual phases. The Pb was principally combined with the primary minerals in raw SS. However, the percentages in the directly toxic category (F1 + F2) of Zn, Ni, and Cd reached (56.5, 49.7, and 42.1) %, respectively, indicating the high environmental risk from Zn, Ni, and Cd in raw SS if applied to the soil.

In relation to the HM fractions in raw SS, a remarkable decrease of the F1 and F2 fractions occurred in the SRs (Fig. 3). For Zn, Ni, and Cd in the SRs, the F1 and F2 fractions decreased from (56.5, 49.7, and 42.1) % in the SS, to less than (35.6, 29.5, and 27.3) %, respectively. Accordingly, the F4 fraction of these HMs, and the F3 fraction of Zn, increased. It was inferred from the above results that hydrothermal treatment had some effect on the immobilization of HMs because the bioavailable fractions (F1 and F2) can migrate into the most stable fraction (F4) during the hydrothermal treatment process. Results from previous studies indicated that some interactions (i.e. adsorption, precipitation, and complexation) might occur between the HMs and the crystal lattices of the SS, especially at hydrothermal treatment temperatures higher than 200 °C (Pan, 2010; Shi et al., 2013). However, the percentages in the directly

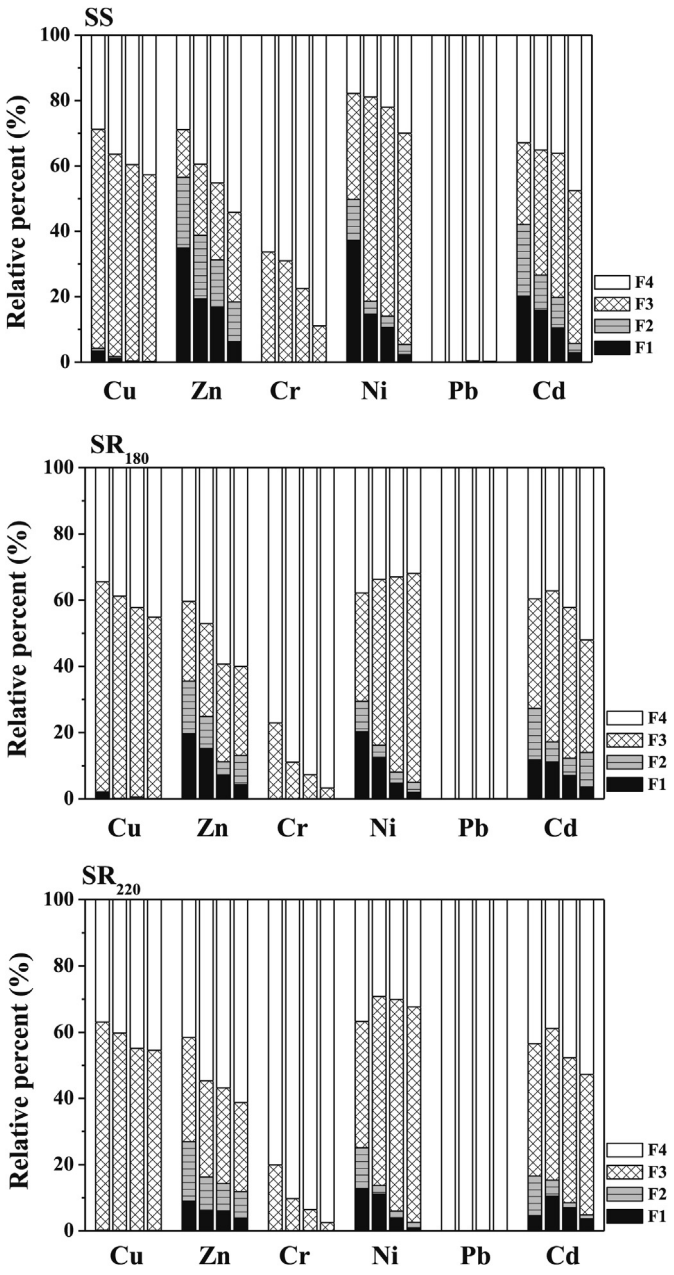

Fig. 3. Fraction distribution of heavy metals in SS, SR_{180}, SR_{220}, and their biochars formed at (300, 500, and 700) °C, respectively. SS, sewage sludge; SR_{180}, the solid residue obtained from hydrothermal treatment sewage sludge at 180 °C; SR_{220}, the solid residue obtained from hydrothermal treatment sewage sludge at 220 °C.

toxic category (F1 + F2) of Zn, Ni, and Cd in SR remained high and constituted threats due to their potential bioavailability and ecotoxicity.

Fig. 3 also shows the speciation of HMs in the biochars derived from SS and SRs. It can be observed that a sharp drop occurred in the percentage of the directly toxic category (F1 + F2) of HMs after conversion of the SS/SR to biochar via pyrolysis at higher temperatures. This implies a sharp decline in the environmental risk from biochar due to rapid increase in the stable fraction (F4) of HMs in biochar with rise in the pyrolysis temperature. For example, the percentage of Zn, Ni, and Cd in the bioavailable fraction (F1 + F2) in the SS biochar significantly decreased from (38.8, 18.6, and 26.6) % to (18.4, 5.4, and 5.7) %, respectively, with rise of the pyrolysis temperature from 300 to 700 °C. In accordance, the percentage of Zn, Ni, Cd, Cu, and Cr in the F4 fraction in SS biochar formed at 700 °C increased greatly to (54.2, 29.9, 47.5, 42.7, and 88.9) %, respectively. This indicated that high pyrolysis temperature is a key factor for immobilization of HMs in the biochar (Shao et al., 2015). The species of Pb in biochar also showed no obvious change and was mainly present in F4 (nearly 100%). These results show that the directly toxic and bioavailable fractions (F1 and F2) of the HMs in the SS decreased significantly as a result of pyrolysis technology, indicating that the pyrolysis technology had significant effect on the immobilization of the HMs. Surprisingly, after pyrolytic conversion of SR to biochar, the percentage of the bioavailable fraction (F1 + F2) of HMs in the SR biochar decreased dramatically with increasing pyrolysis temperature. The percentage of F3 and F4 fractions of HMs in SR biochar also increased steadily. Furthermore, conversion of SR to biochar could further promote transformation of the bioavailable fraction (F1 + F2) of HMs to the more stable F3 or F4 fractions, resulting in enhanced immobilization of the HMs in SS. This suggests that the HTP technology was the best method for immobilization of HMs in SS, when compared with hydrothermal treatment alone or pyrolysis alone.

3.4.3. Risk analysis of HMs

The risk assessment codes (RAC) of Cu, Zn, Cr, Ni, Pb, and Cd in the raw SS, SR, and their biochar samples, are displayed in Table 3. It can be seen that the Cr, Pb, and Cu in the raw SS, SR, and their biochar samples possess no-risk or low-risk levels, indicating low toxicity to the environment. In other words, the risk levels of Cr, Pb, and Cu in the SS changed very little after treatment using the proposed processing technologies. This is because the percentage of F1 and F2 fractions for Cr, Pb, and Cu in SS was very low (Fig. 3). The risk of Cd in raw SS, SR_{180}, SSC-300 and SRC_{180}-300 were assessed to be of medium risk. After hydrothermal treatment and pyrolysis at high temperature, the risks from Cd in SR_{220} and in the biochars obtained at higher pyrolysis temperature (≥500 °C), changed to low. This showed that the risk from Cd in raw SS was essentially eliminated after high-temperature thermal treatment. Zn and Ni in raw SS were considered high-risk, indicating potentially high environmental toxicity. The risk of Zn and Ni in the SRs were still medium risk, except for Zn in SR_{220}. However, it was noticed that the environmental risk of Zn and Ni in SS was transformed from high risk to medium risk or low risk in the biochars obtained by the pyrolysis process. Previous studies also indicated that both hydrothermal treatment and pyrolysis technologies have positive benefits in reducing the risk of HMs in SS. This has made these processes increasingly attractive due to their environmental

Table 3
Risk assessment codes of HMs in SS, SR, and biochar.

Samples	Cu	Zn	Cr	Ni	Pb	Cd
SS	3.44/LR	34.96/HR	0.00/NR	37.28/HR	0.00/NR	20.18/MR
SS-300	1.25/LR	19.33/MR	0.00/NR	14.61/MR	0.00/NR	15.81/MR
SS-500	0.13/NR	16.87/MR	0.00/NR	10.60LR	0.00/NR	10.41/LR
SS-700	0.12/NR	6.31/LR	0.00/NR	2.36LR	0.04/NR	2.94/LR
SR_{180}	1.73/LR	19.69/MR	0.00/NR	20.23/MR	0.00/NR	11.80/MR
SR_{180}-300	0.00/NR	15.19/MR	0.00/NR	12.50/MR	0.00/NR	11.18/MR
SR_{180}-500	0.00/NR	7.27/LR	0.00/NR	4.74/LR	0.00/NR	7.10/LR
SR_{180}-700	0.10/NR	4.34/LR	0.00/NR	2.01/LR	0.03/NR	3.50/LR
SR_{220}	0.11/NR	9.02/LR	0.00/NR	12.78/MR	0.00/NR	4.55/LR
SR_{220}-300	0.00/NR	6.18/LR	0.00/NR	11.04/MR	0.00/NR	10.43/LR
SR_{220}-500	0.00/NR	6.03/LR	0.00/NR	3.94/LR	0.00/NR	6.97/LR
SR_{220}-700	0.10/NR	3.87/LR	0.00/NR	0.95/LR	0.02/NR	3.64/LR

SS, sewage sludge; SR_X, the solid residue obtained from hydrothermal treatment sewage sludge at X (°C) temperature; SSC-Y, biochar derived from sewage sludge pyrolysis at Y (°C) temperature; SRC_X-Y, biochar derived from hydrothermally treated sewage sludge at X (°C) pyrolysis at Y (°C) temperature.

Table 4
Ecological risk assessment of the HMs in SS, SR, and biochar.

Sample	C_r						E_r						RI
	Cu	Zn	Cr	Ni	Pb	Cd	Cu	Zn	Cr	Ni	Pb	Cd	
SS	2.48	2.47	1.17	2.86	0.00	2.33	12.38	2.47	2.34	17.14	0.00	70.02	104.36
SSC-300	1.75	1.66	0.85	2.23	0.00	1.78	8.74	1.66	1.70	13.37	0.00	53.50	78.98
SSC-500	1.52	1.38	0.57	1.97	0.01	1.61	7.62	1.38	1.14	11.81	0.06	48.36	70.37
SSC-700	1.34	1.07	0.26	1.64	0.01	1.23	6.71	1.07	0.52	9.84	0.03	36.85	55.02
SR_{180}	1.90	1.73	0.67	1.80	0.00	1.75	9.50	1.73	1.33	10.81	0.01	52.53	75.91
SRC_{180}-300	1.58	1.36	0.29	1.71	0.00	1.62	7.88	1.36	0.57	10.24	0.00	48.54	68.60
SRC_{180}-500	1.37	0.96	0.17	1.59	0.00	1.37	6.84	0.96	0.35	9.52	0.02	41.09	58.78
SRC_{180}-700	1.21	0.89	0.07	1.51	0.00	1.06	6.07	0.89	0.15	9.04	0.02	31.85	48.01
SR_{220}	1.71	1.58	0.54	1.71	0.00	1.53	8.54	1.58	1.08	10.28	0.00	45.93	67.41
SRC_{220}-300	1.49	1.13	0.24	1.76	0.00	1.52	7.43	1.13	0.48	10.56	0.00	45.60	65.20
SRC_{220}-500	1.23	0.96	0.14	1.56	0.00	1.17	6.14	0.96	0.29	9.35	0.02	34.95	51.71
SRC_{220}-700	1.20	0.85	0.06	1.49	0.00	1.04	6.00	0.85	0.11	8.93	0.01	31.21	47.12

SS, sewage sludge; SR_X, the solid residue obtained from hydrothermal treatment sewage sludge at X (°C) temperature; SSC-Y, biochar derived from sewage sludge pyrolysis at Y (°C) temperature; SRC_X-Y, biochar derived from hydrothermally treated sewage sludge at X (°C) pyrolysis at Y (°C) temperature.

compatibility (Leng et al., 2014; Shao et al., 2015). Furthermore, after the HTP process at high temperature (≥500 °C), Cr, Pb, and Cu in SR-biochars presented no risk, and the risks from of Cd, Zn, and Ni also became low.

Potential ecological risk index (RI) results for HMs in SS, SRs, and their biochar samples are shown in Table 4. It can be noticed that the value of RI for the SS is 104.36, indicating a high degree of HMs contamination. The values of RI for the SRs and biochars are decreased with increasing of hydrothermal temperature and pyrolysis temperature. Remarkably, the biochars obtained from HTP process at a high temperature (≥500 °C) are assessed to the lowest risk. Therefore, the above results indicated that the HTP method was found to be an effective and feasible technology for the safe treatment of wet SS.

4. Conclusions

In this study, a new concept was presented for combining hydrothermal pretreatment with pyrolysis (HTP) for SS treatment and disposal. Wet SS was first given a hydrothermal pretreatment; then the obtained solid was pyrolyzed to prepare SS-derived biochar at temperatures from 300 to 700 °C. The use of a single hydrothermal treatment and pyrolysis alone, were investigated for comparison. The effects of pyrolysis temperature on the characteristics of biochar and the risk assessment of HMs in biochar were also estimated.

The characteristics of SS-derived biochar, such as the biochar yield, pH value, ash content, functional groups, aromatic content, surface characterizations, and micromorphology were significantly affected by pyrolysis temperature. Moreover, there was a sharp increase in the N_2 adsorption capacity and BET surface area after SR_{220} was subjected to pyrolysis at 500 °C. Furthermore, the SC_{220}-500 sample achieved the maximum possible results. Compared with hydrothermal treatment and pyrolysis, the HTP process at higher temperature can better promote transformation of the bioavailable fraction (F1 + F2) of HMs to the more stable F3 and F4 fractions. The result is that the potential environmental risk of the HMs in SS was transformed from high-risk to low-risk, or even no-risk. These results indicate that the HTP process seems an effective and promising technology not only for enhancing the quality of SS-derived biochar, but also for reducing the toxicity and environmental risk of the HMs in SS.

Acknowledgments

This work was supported by the China-Japan Research Cooperative Program [Grant No. 2016YFE0118000]; the National Natural Science Foundation of China [Grant No. 41373092]; the Key Project of Young Talent of Institute of Urban Environment,Chinese Academy of Sciences (IUE, CAS) [Grant No. IUEZD201402]; the Scientific and Technological Major Special Project of Tianjin City [Grant No. 16YFXTSF00420]; the Industry Leading Key Projects of Fujian Province [Grant No. 2015H0044], and the Key Project of Young Talents Frontier of Institute of Urban Environment,Chinese Academy of Sciences (IUE, CAS) [Grant No. IUEQN201501].

Appendix A. Supplementary data

Supplementary data to this article can be found online at https://doi.org/10.1016/j.chemosphere.2018.10.189.

References

Agrafioti, E., Bouras, G., Kalderis, D., Diamadopoulos, E., 2013. Biochar production by sewage sludge pyrolysis. J. Anal. Appl. Pyrolysis 101, 72–78.
Akiya, N., Savage, P.E., 2002. Roles of water for chemical reaction in high temperature water. Chem. Rev. 102, 2725–2750.
Bougrier, C., Delgenès, J.P., Carrère, H., 2008. Effects of thermal treatments on five different waste activated sludge samples solubilisation, physical properties and anaerobic digestion. Chem. Eng. J. 139, 236–244.
Cayuela, M.L., Jeffery, S., Van Zwieten, L., 2015. The molar H:Corg ratio of biochar is a key factor in mitigating N2O emissions from soil. Agric. Ecosyst. Environ. 202, 135–138.
Chen, B., Zhou, D., Zhu, L., 2008a. Transitional adsorption and partition of nonpolar and polar aromatic contaminants by biochars of pine needles with different pyrolytic temperatures. Environ. Sci. Technol. 42, 5137–5143.
Chen, H., Yan, S.H., Ye, Z.L., Meng, H.J., Zhu, Y.G., 2012. Utilization of urban sewage sludge: Chinese perspectives. Environ. Sci. Pollut. Res. Int. 19, 1454–1463.
Chen, M., Li, X.M., Yang, Q., Zeng, G.M., Zhang, Y., Liao, D.X., Liu, J.J., Hu, J.M., Guo, L., 2008b. Total concentrations and speciation of heavy metals in municipal sludge from Changsha, Zhuzhou and Xiangtan in middle-south region of China. J. Hazard Mater. 160, 324–329.
Chen, T., Zhang, Y., Wang, H., Lu, W., Zhou, Z., Zhang, Y., Ren, L., 2014. Influence of pyrolysis temperature on characteristics and heavy metal adsorptive performance of biochar derived from municipal sewage sludge. Bioresour. Technol. 164, 47–54.
Devi, P., Saroha, A.K., 2014. Risk analysis of pyrolyzed biochar made from paper mill effluent treatment plant sludge for bioavailability and eco-toxicity of heavy metals. Bioresour. Technol. 162, 308–315.
Funke, A., Ziegler, F., 2010. Hydrothermal carbonization of biomass: a summary and discussion of chemical mechanisms for process engineering. Biofuel. Bioprod. Bioref. 4, 160–177.
Garlapalli, R.K., Wirth, B., Reza, M.T., 2016. Pyrolysis of hydrochar from digestate: effect of hydrothermal carbonization and pyrolysis temperatures on pyrochar formation. Bioresour. Technol. 220, 168–174.
Hakanson, L., 1980. An ecological risk index for aquatic pollution control. A sedimentological approach. Water. Res. 14, 975–1001.
Han, J., Wang, X., Yue, J., Gao, S., Xu, G., 2014. Catalytic upgrading of coal pyrolysis tar over char-based catalysts. Fuel Process. Technol. 122, 98–106.
Harvey, O.R., Herbert, B.E., Rhue, R.D., Kuo, L.J., 2011. Metal interactions at the biochar-water interface: energetics and structure-sorption relationships

elucidated by flow adsorption microcalorimetry. Environ. Sci. Technol. 45, 5550–5556.
Havukainen, J., Zhan, M., Dong, J., Liikanen, M., Deviatkin, I., Li, X., Horttanainen, M., 2017. Environmental impact assessment of municipal solid waste management incorporating mechanical treatment of waste and incineration in Hangzhou, China. J. Clean. Prod. 141, 453–461.
Hayes, T.D., Theis, T.L., 1978. The distribution of heavy metals in anaerobic digestion. J. Water Pollut. Control Fed. 61–72.
He, C., Giannis, A., Wang, J.Y., 2013. Conversion of sewage sludge to clean solid fuel using hydrothermal carbonization: hydrochar fuel characteristics and combustion behavior. Appl. Energy 111, 257–266.
Ho, S.H., Yang, Z.K., Nagarajan, D., Chang, J.S., Ren, N.Q., 2017. High-efficiency removal of lead from wastewater by biochar derived from anaerobic digestion sludge. Bioresour. Technol. 246, 142–149.
Hossain, M.K., Strezov, V., Chan, K.Y., Ziolkowski, A., Nelson, P.F., 2011. Influence of pyrolysis temperature on production and nutrient properties of wastewater sludge biochar. J. Environ. Manag. 92, 223–228.
Huang, H.J., Yang, T., Lai, F.Y., Wu, G.Q., 2017. Co-pyrolysis of sewage sludge and sawdust/rice straw for the production of biochar. J. Anal. Appl. Pyrolysis 125, 61–68.
Huang, H.J., Yuan, X.Z., 2016. The migration and transformation behaviors of heavy metals during the hydrothermal treatment of sewage sludge. Bioresour. Technol. 200, 991–998.
Jin, J., Li, Y., Zhang, J., Wu, S., Cao, Y., Liang, P., Zhang, J., Wong, M.H., Wang, M., Shan, S., Christie, P., 2016. Influence of pyrolysis temperature on properties and environmental safety of heavy metals in biochars derived from municipal sewage sludge. J. Hazard Mater. 320, 417–426.
Khan, S., Chao, C., Waqas, M., Arp, H.P.H., Zhu, Y.G., 2013. Sewage sludge biochar influence upon rice (Oryza sativa L) yield, metal bioaccumulation and greenhouse gas emissions from acidic paddy soil. Environ. Sci. Technol. 47, 8624–8632.
Kistler, R.C., Widmer, F., Brunner, P.H., 1987. Behavior of chromium, nickel, copper, zinc, cadmium, mercury, and lead during the pyrolysis of sewage sludge. Environ. Sci. Technol. 21, 704–708.
Leng, L., Yuan, X., Huang, H., Jiang, H., Chen, X., Zeng, G., 2014. The migration and transformation behavior of heavy metals during the liquefaction process of sewage sludge. Bioresour. Technol. 167, 144–150.
Leng, L., Yuan, X., Shao, J., Huang, H., Wang, H., Li, H., Chen, X., Zeng, G., 2016. Study on demetalization of sewage sludge by sequential extraction before liquefaction for the production of cleaner bio-oil and bio-char. Bioresour. Technol. 200, 320–327.
Li, H., Mahyoub, S.A.A., Liao, W., Xia, S., Zhao, H., Guo, M., Ma, P., 2017. Effect of pyrolysis temperature on characteristics and aromatic contaminants adsorption behavior of magnetic biochar derived from pyrolysis oil distillation residue. Bioresour. Technol. 223, 20–26.
Liu, W.J., Li, W.W., Jiang, H., Yu, H.Q., 2017. Fates of chemical elements in biomass during its pyrolysis. Chem. Rev. 117, 6367–6398.
Lu, H., Zhang, W., Wang, S., Zhuang, L., Yang, Y., Qiu, R., 2013. Characterization of sewage sludge-derived biochars from different feedstocks and pyrolysis temperatures. J. Anal. Appl. Pyrolysis 102, 137–143.
Mendez, A., Paz-Ferreiro, J., Araujo, F., Gasco, G., 2014. Biochar from pyrolysis of deinking paper sludge and its use in the treatment of a nickel polluted soil. J. Anal. Appl. Pyrolysis 107, 46–52.
Mumme, J., Titirici, M.M., Pfeiffer, A., Lüder, U., Reza, M.T., Mašek, O., 2015. Hydrothermal carbonization of digestate in the presence of zeolite: process efficiency and composite properties. ACS Sustain. Chem. Eng. 3, 2967–2974.
Pan, H., 2010. Effects of liquefaction time and temperature on heavy metal removal and distribution in liquefied CCA-treated wood sludge. Chemosphere 80, 438–444.
Peng, C., Zhai, Y., Zhu, Y., Xu, B., Wang, T., Li, C., Zeng, G., 2016. Production of char from sewage sludge employing hydrothermal carbonization: char properties, combustion behavior and thermal characteristics. Fuel 176, 110–118.
Qayyum, M.F., Steffens, D., Reisenauer, H.P., Schubert, S., 2014. Biochars influence differential distribution and chemical composition of soil organic matter. Plant Soil Environ. 60, 337–343.
Reza, M.T., Uddin, M.H., Lynam, J.G., Hoekman, S.K., Coronella, C.J., 2014. Hydrothermal carbonization of loblolly pine: reaction chemistry and water balance. Biomass Convers. Bioresourc. 4, 311–321.
Schwarzenbach, R.P., Escher, B.I., Fenner, K., Hofstetter, T.B., Johnson, C.A., Von Gunten, U., Wehrli, B., 2006. The challenge of micropollutants in aquatic systems. Science 313, 1072–1077.
Shao, J., Yuan, X., Leng, L., Huang, H., Jiang, L., Wang, H., Chen, X.,G., 2015. The comparison of the migration and transformation behavior of heavy metals during pyrolysis and liquefaction of municipal sewage sludge, paper mill sludge, and slaughterhouse sludge. Bioresour. Technol. 198, 16–22.
Shi, W., Liu, C., Ding, D., Lei, Z., Yang, Y., Feng, C., Zhang, Z., 2013. Immobilization of heavy metals in sewage sludge by using subcritical water technology. Bioresour. Technol. 137, 18–24.
Sohi, S.P., 2012. Carbon storage with benefits. Science 338, 1034–1035.
Staelens, N., Parkpian, P., Polprasert, C., 2000. Assessment of metal speciation evolution in sewage sludge dewatered in vertical flow reed beds using a sequential extraction scheme. Chem. Speciat. Bioavailab. 12, 97–107.
Wang, X., Li, C., Zhang, B., Lin, J., Chi, Q., Wang, Y., 2016. Migration and risk assessment of heavy metals in sewage sludge during hydrothermal treatment combined with pyrolysis. Bioresour. Technol. 221, 560–567.
Wong, J.W.C., Li, K., Fang, M., Su, D.C., 2001. Toxicity evaluation of sewage sludges in Hong Kong. Environ. Int. 27, 373–380.
Xiao, X., Chen, B., 2017. A direct observation of the fine aromatic clusters and molecular structures of biochars. Environ. Sci. Technol. 51, 5473–5482.
Yuan, J.H., Xu, R.K., Zhang, H., 2011a. The forms of alkalis in the biochar produced from crop residues at different temperatures. Bioresour. Technol. 102, 3488–3497.
Yuan, X., Huang, H., Zeng, G., Li, H., Wang, J., Zhou, C., Zhu, H., Pei, X., Liu, Z., Liu, Z., 2011b. Total concentrations and chemical speciation of heavy metals in liquefaction residues of sewage sludge. Bioresour. Technol. 102, 4104–4110.
Yue, Y., Cui, L., Lin, Q., Li, G., Zhao, X., 2017. Efficiency of sewage sludge biochar in improving urban soil properties and promoting grass growth. Chemosphere 173, 551–556.
Zhai, Y., Chen, H., Xu, B., Xiang, B., Chen, Z., Li, C., Zeng, G., 2014. Influence of sewage sludge-based activated carbon and temperature on the liquefaction of sewage sludge: yield and composition of bio-oil, immobilization and risk assessment of heavy metals. Bioresour. Technol. 159, 72–79.
Zhang, J.H., Lin, Q.M., Zhao, X.R., 2014. The hydrochar characters of municipal sewage sludge under different hydrothermal temperatures and durations. J. Integr. Agric. 13, 471–482.
Zheng, H., Wang, Z., Deng, X., Zhao, J., Luo, Y., Novak, J., Herbert, S., Xing, B., 2013. Characteristics and nutrient values of biochars produced from giant reed at different temperatures. Bioresour. Technol. 130, 463–471.